Reconstruction of Compressed Sensing MRI by Computing Finite Differences of Wavelet Coefficients

Md Mashud Hyder[1,2], Bradley Peterson[1,2], and Zhengchao Dong[1,2]
[1]*Brain Imaging Lab, Columbia University, New York, NY, United States,* [2]*New York State Psychiatric Inst., New York, NY, United States*

INTRODUCTION: The application of compressed sensing (CS) to MRI has the potential to reduce data actuation time significantly [1]. The theory of CS states that MRI images can be recovered efficiently from randomly undersampled k-space data under certain conditions, mainly sparsity and compressibility in certain transformed domains [1-3]. Many MRI images have sparse representation when we calculate their spatial finite-differences or wavelet coefficients. In this work we show that spatial finite-differences of a set of wavelet coefficients can increase the sparsity of MRI image, which results in improved recovery of CS MRI.

METHODS: To recover MRI image from randomly undersampled k-space data, the following optimization algorithm was used in [1],

$$\min_x \| \phi(x) \|_1 + \alpha \| TV(x) \|_1, s.t. \| F_u(x) - y \|_2 < \varepsilon \quad (1)$$

where $x \in C^{n \times n}$ represents the image of interest, ϕ denotes wavelet basis, F_u is the undersampled Fourier basis, y is the measured k-space data, $\| x \|_1$ indicates l_1 norm, TV is the total-variation operator, which calculates the sum of absolute variations in the image, and α is a weighting parameter. In particular, TV represents spatial finite-differences of the image. However, there are two problems with this formulation: i) one needs to compute both wavelet coefficients and TV of the full image in every iteration, and ii) the value of α depends on the problem under consideration. Now, we let $z=\phi(x)$ and construct $z_l \in C^{l \times l}$ from z by selecting the coefficients of the lowpass wavelet filter outputs (Fig 1(a), (b)). We see that z_l is not sparse (Fig 1(c)), but $TV(z_l)$ is significantly sparse (Fig 1(d)). Based on this idea we propose a new formulation. We set the values of the coefficients of the lowpass wavelet filter outputs in z to zero and consider the following optimization problem:

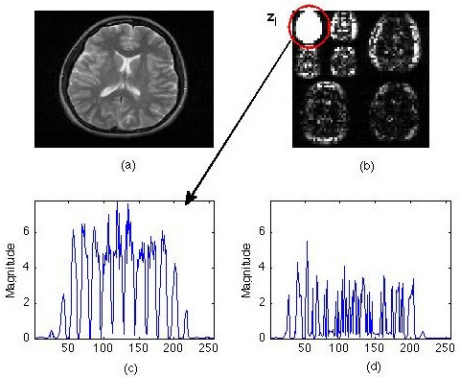

Figure 1: (a) Axial brain image, (b) 2-D wavelet transform, (c) pattern of z_l, (d) pattern of $TV(z_l)$.

$$\min_x \| z \|_0 + \| TV(z_l) \|_0 + \lambda \| F_u(x) - y \|_2 \quad (2)$$

where the value of λ depends on noise. The optimization procedure proposed in [4], where a Gaussian family of functions was used to approximate the l_0 norm, was used to solve (2). In the image reconstruction, we set $\lambda=10^5$ in Eq. (2) for the proposed method and used $\alpha=0.01$ in Eq. (1) for the method we denoted as ALGO-1. We used the k-space dataset provided in [1] and the Shepp-Logan phantom for performance evaluation. The data in [1] were axial brain images acquired on a 1.5T Signa Excite scanner and the dimension of all images were 256×256. The simulations for optimizing (1) and (2) were performed in MATLAB7 environment using an Intel Core 2 Duo, 2.66 GHz processor with 4GB of memory, under Mac OS X Version 10.5.5 operating system.

RESULTS AND DISCUSSION: We first considered axial brain image reconstruction from 5x undersampled k-space data (Fig 2). The zero-filling (ZF) and ALGO-1 reconstructions were unable to reveal the details of the brain image (Fid 2 (c)), while most of the critical edges and features of the brain image were recovered by the proposed method (Figure 2(d)). The Shepp-Logan phantom image in Fig 3(a) was also subjected to a random 5x undersampling. As expected, the reconstruction by using the proposed algorithm was better compared to the other two algorithms. We then investigated the recovery performance of Shepp-Logan phantom by different algorithms under different undersampled rates in Fig 4. In every undersampled situation the images were reconstructed by different algorithms and their root mean squired error (RMSE) were calculated. When the sample size was small, ie, the undersampling rate was large, the proposed algorithm performed significantly better than ALGO-1. In Fig 4, the RMSE of the proposed algorithm and ALGO-1 were 0.058 and 0.097, respectively, with 15% k-space data. Hence, the RMSE difference was 0.039. However, when sample size increased to 35%, the RMSE of the two algorithms were 0.018 and 0.035, respectively. Hence performance gap of the two algorithms deceased with increasing sample size.

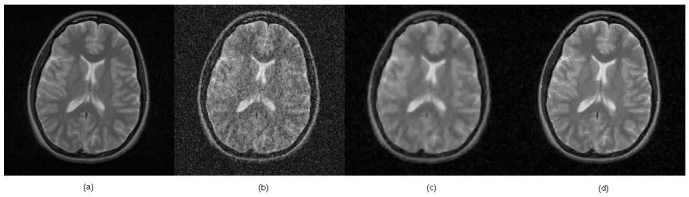

Figure 2: Fully sampled image (a) and images reconstructed from 5x under-sampled data by ZF-w/dc (b), ALGO-1 (c), and the proposed algorithm (d).

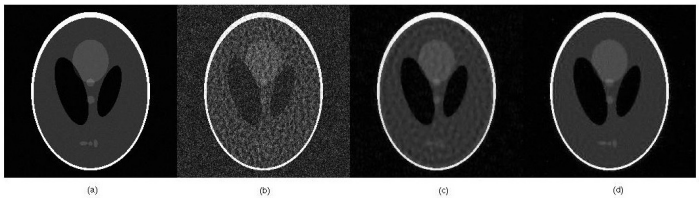

Figure 3: Shepp-Logan phantom (a) reconstruction from 5x undersampled k-space data by ZF-w/dc (b), ALGO-1 (c), and the proposed algorithm (d).

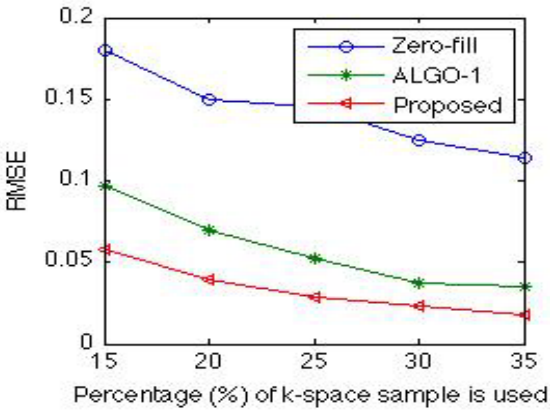

Figure 4: RMSE vs percentage of undersampled data for different algorithms.

REFERENCES: [1] M. Lustig, et al., Magn Reson Med. 58, 1182-1195, 2007. [2] S. Ravishankar, et al., IEEE Trans. Medical Imaging, 1028 - 1041, 2011. [3] J.P. Halder, et al., IEEE Trans. Medical Imaging, 893 – 903, 2011. [4] M. Hyder, et al., IEEE Trans Signal Processing, 2194 – 2205, 2010.